Ultrathin NiO nanoflakes perpendicularly oriented on carbon nanotubes as lithium ion battery anode

Jialiang Zhong
School of Chemistry and Chemical Engineering, Xinjiang University, Urumqi 830046, People's Republic of China

Oh B. Chae
Department of Chemical and Biological Engineering and World Class University (WCU) program of Chemical Convergence for Energy & Environment (C_2E_2), Seoul National University, Seoul 151-744, Korea

Wei Shi, Jianzhang Fan, and Hongyu Mi[a)]
School of Chemistry and Chemical Engineering, Xinjiang University, Urumqi 830046, People's Republic of China

Seung Mo Oh[b)]
Department of Chemical and Biological Engineering and World Class University (WCU) program of Chemical Convergence for Energy & Environment (C_2E_2), Seoul National University, Seoul 151-744, Korea

(Received 23 April 2013; accepted 15 July 2013)

Core–shell nickel oxide/carbon nanotube (CNT) microwires, with interconnected nickel oxide nanoflakes (~10 nm in thickness) vertically oriented on polymer-based CNTs, were synthesized by using low-cost starting materials and a scalable growth route. As revealed by morphological characterization, sheet–sheet and wire–wire interwoven of the composite constructed a porous structure. The composite as lithium ion battery anode exhibited high reversible capacity of 752 mAh/g at a current density of 100 mA/g over 30 cycles with 82% capacity retention. Even at high rate (1000 mA/g), the composite still delivered a high charge capacity (304 mAh/g) over 25 cycles. When the rate was reset to its initial value, 87.7% of the initial charge capacity was recovered. The composite showed remarkably enhanced performance compared to pure NiO, which was presumably due to the advantages of porous structure, oriented attachment, and attractive synergetic effect.

I. INTRODUCTION

Designing and developing high-performance anode materials with higher power and energy densities are especially significant for the scale-up applications of lithium ion batteries (LIBs) in electric vehicles, plug-in hybrid electric vehicles, and large energy storage devices.[1–6] Nickel oxide (NiO) anode as a candidate of the commercially available graphite possesses advantages of high theoretical capacity (~718 mAh/g), low cost, and environmental benignity, and thus represents a kind of promising material in LIBs. However, NiO endures poor cycle performance because large volume change caused by conversion reactions between NiO and lithium may lead to electrode pulverization and electrical detachment.[7–10] Additionally, poor electronic/ionic conductivities also limit the application of NiO anode. Therefore, various strategies are attempted to overcome those disadvantages, in which compounding nanostructured NiO with some conductive buffer matrix is demonstrated to be an effective approach.[11–22] Especially, NiO-based nanocomposites, that are assembled from one-dimensional (1D) carbon nanotubes (CNTs) or two-dimensional (2D) graphene sheets and 1D NiO nanoparticles or 2D NiO nanosheets, represent ideal architectures with some merits such as large liquid–solid interface area, short diffusion path for Li^+ diffusion, high electronic conductivity for fast electron transfer, and effective cushion against severe volumetric expansion during repeated cycling.[16–22] For example, crystallized NiO/MWCNT nanocomposites reported by Xu et al.[20] had a discharge capacity of ~800 mAh/g at 50 mA/g over 50 discharge/charge cycles. NiO nanoplates grown on graphene synthesized by Hwang et al.[21] were capable of delivering the maximum discharge capacity of 856 mAh/g with superior rate properties and cycle performance. Zhou et al.[22] prepared a composite of 2D NiO nanosheets anchored strongly on 2D graphene sheets through a C–O–Ni bridge, which exhibited attracting lithium storage capability. However, rare studies have been reported on the composites consisting of 1D carbon materials and 2D oxide nanoflakes so far, which still remains a challenge in terms of synthetic method and lithium storage performance.

In this work, core/shell composites consisting of 2D NiO nanoflakes and 1D polypyrrole-based carbon nanotubes (PCNTs) have been prepared through a convenient pH-controlled approach, followed by heat treatment under inert atmosphere. The as-prepared composite is morphologically, structurally, and electrochemically

Address all correspondence to these authors.
[a)]e-mail: mmihongyu@163.com
[b)]e-mail: seungoh@plaza.snu.ac.kr
DOI: 10.1557/jmr.2013.227

 © Materials Research Society 2013

https://doi.org/10.1557/jmr.2013.227 Published online by Cambridge University Press

characterized by transmission electron microscopy, scanning electron microscopy, x-ray diffraction (XRD), and electrochemical tests. Results indicate that porous NiO/PCNT composites have high capacity, good cycling performance, and rate capability.

II. EXPERIMENT

All the reagents were used as received unless otherwise stated. Fresh pyrrole (Py, 99%, Aldrich Chemical Co., Milwaukee, WI) by distillation was used. For pure NiO, an ammonia hydroxide solution (5%) was added slowly into 100 mL of 0.2 M nickel chloride ($NiCl_2$) solution until the pH $\approx$ 9.5 followed by further stirring for another 24 h. The green precipitate was collected by being filtered and washed with deionized water and ethanol several times. After being dried at 80 °C overnight, the precipitate was thermally transferred into pure NiO at 250 °C under inert atmosphere for 2 h with a heating rate of 10 °C/min. To investigate the morphology evolution of nickel hydroxide [$Ni(OH)_2$], various $Ni(OH)_2$ precursors with pH values of 8.5, 9.0, 9.5, and 10.0 were prepared. The preparation of $Ni(OH)_2$/PCNT precursor resembled the described method with a change of pH value (pH $\approx$ 9.5).[23] The $Ni(OH)_2$/PCNT was then heated at 250 °C under inert atmosphere for 2 h to generate the NiO/PCNT composite.

Morphological characterization was performed on a Supra 55VP field-emission scanning electron microscope (SEM; Carl Zeiss, Oberkochen, Germany) and a Hitachi 600 transition electron microscope (TEM; Hitachi Co., Tokyo, Japan), respectively. The powder XRD pattern was recorded using a Bruker D8 x-ray diffractometer (Bruker AXS GmbH, Karlsruhe, Germany) with a Cu K_α radiation (λ = 0.154056 nm). Thermogravimetric analysis (TGA) was conducted on a Netzsch DSC 200 F3 thermogravimetric analyzer (NETZSCH-Gerätebau GmbH, Selb, Germany) with a heating rate of 10 °C/min from 25 to 900 °C in air.

The working electrode was made by mixing active material, super P, and polyvinylidene fluoride at a mass ratio of 80:10:10 in N-methyl pyrrolidinone. This mixture slurry was coated on a copper foil, dried, and roll-pressed. This foil was then cut into circular disks, and vacuum-dried at 120 °C for 12 h. The loading of active materials is about 0.5 mg. Anodic performance was evaluated on TOSCAT-3100 battery cycler (Toyo system, Tachikawa-Shi, Tokyo, Japan) using coin-typed half cells assembled in an argon-filled glovebox. Lithium foil was used as the counter electrode. The electrolyte consisted of 1 M lithium hexafluorophosphate ($LiPF_6$) solution in an ethylene carbonate/dimethyl carbonate mixture (1:2, V/V). The assembled cells were cycled between 0.01 and 3 V (versus Li/Li^+).

III. RESULTS AND DISCUSSION

Typical morphology evolution of $Ni(OH)_2$ precursors is presented in Fig. 1. Versatile variation in morphology can be conveniently controlled by the alteration of pH values.

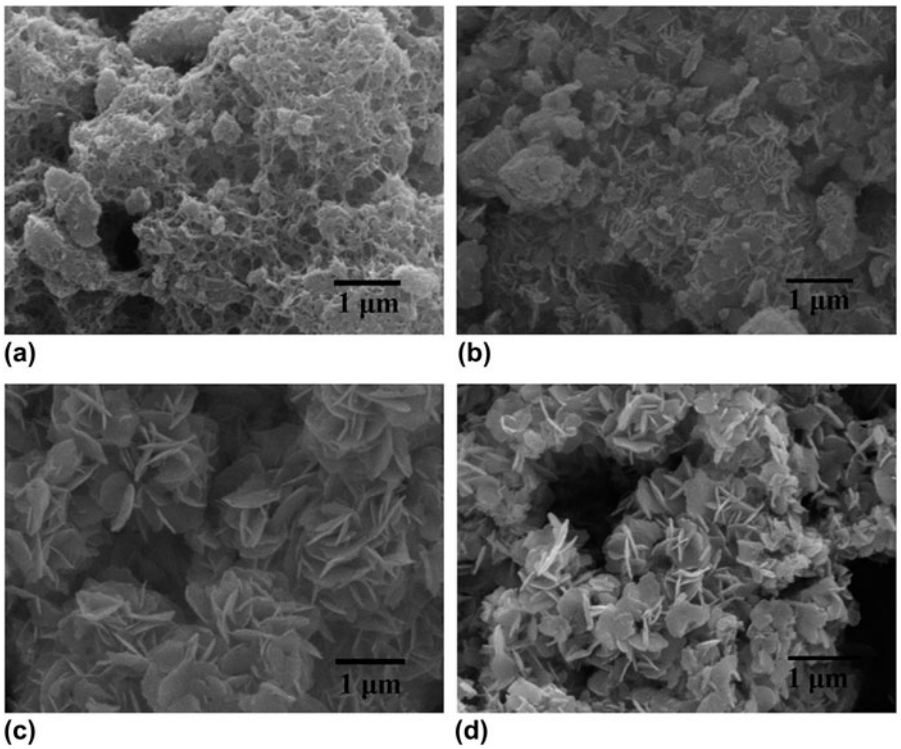


FIG. 1. Typical SEM images showing the morphology evolution of $Ni(OH)_2$ precursors under different pH values: (a) 8.5, (b) 9, (c) 9.5, and (d) 10.

https://doi.org/10.1557/jmr.2013.227 Published online by Cambridge University Press

As shown in Fig. 1, a low pH value of 8.5 leads to the formation of aggregated $Ni(OH)_2$ nanofibers [Fig. 1(a)]. As the pH value increases to 9.0, nanoflake-like morphology can be observed in Fig. 1(b), and a clear nanoflake-stacked flower-like shape can be obtained by increasing the pH value up to 9.5 [Fig. 1(c)]. The size of nanoflakes displays a decreasing tendency with further increase of the pH value [Fig. 1(d)]. Similar phenomenon was reported in the previous literature,[24,25] which might be due to the partial dissolution of $Ni(OH)_2$ to $[Ni(NH_3)_n]^{2+}$ complex based on the following reaction[26]

$$Ni(OH)_2 + nNH_3 \cdot H_2O = [Ni(NH_3)n]^{2+} + 2OH^- + nH_2O \quad .$$

Morphological features of NiO, PCNT, and NiO/PCNT composite are presented in Fig. 2. For pure NiO [Fig. 2(a)], although the flower shape of NiO seems not as apparent as that of the precursor $Ni(OH)_2$, nanoflake morphology with denser packing still remains after thermal decomposition. In comparison with PCNT (~200 nm in diameter) [Fig. 2(b) and its inset], wire-like NiO/PCNT [Fig. 2(c)] has a rough surface with an obvious increase in diameter, suggesting the presence of NiO on PCNT surfaces. Its diameter and length are around 1 μm and several microns, respectively. The magnified SEM image [Fig. 2(d)] clearly illustrates that interconnected ultrathin NiO nanoflakes (~10 nm in thickness) are grown uniformly and vertically on PCNT surfaces to form core/shell wires with nano/micro binary structure. Moreover, sheet–sheet and wire–wire interwoven connection in these microwires generates highly porous structures. According to a previous report, continuous surface-open morphology and preferential orientation of core/shell NiO/PCNT composites can improve both charge/mass transport and mechanical integrity of the electrode, which are beneficial to LIB performance.[27]

The crystalline structures of samples are investigated by XRD patterns, as shown in Fig. 3(a). The main diffraction peaks at 37.2, 43.1, 62.5, and 75.1°, can be easily identified for (111), (200), (220), and (311) crystal planes of the cubic NiO phase, respectively, in accord with JCPDS card no. 47-1049.[28] The strong diffraction peaks indicate high crystallinity of these two samples. Besides, the composite has an additional peak from the (002) plane of hexagonal carbon near 25°.[29] This result indicates that the composite is composed of NiO and carbon. The PCNT content in the composite is analyzed by the TGA curve, as shown in Fig. 3(b). The initial decline of ~4% up to 350 °C is due to the removal of the absorbed water. Another weight loss of ~14.2% occurs between 350 and 600 °C, which is attributed to the burning of PCNT. Accordingly, the composite includes ~14.4% PCNT.

Generally, the structure of the material strongly affects its lithium storage properties. The as-prepared composite

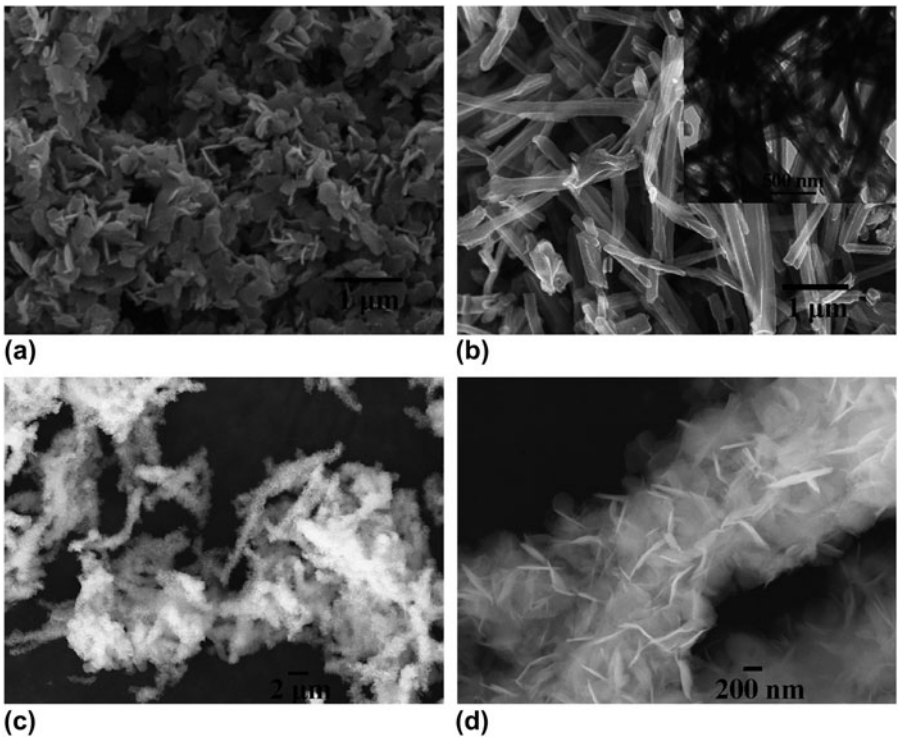


FIG. 2. Typical SEM images of (a) NiO, (b) PCNT, and (c, d) NiO/CNT composite with different magnifications. The inset is the TEM image of PCNT.

https://doi.org/10.1557/jmr.2013.227 Published online by Cambridge University Press

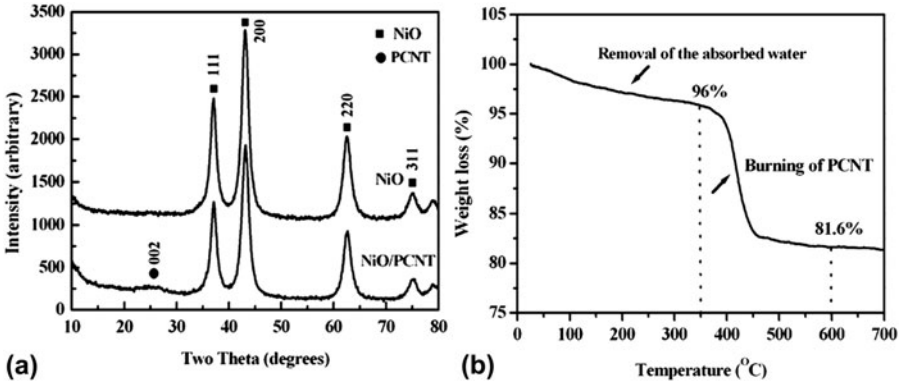


FIG. 3. (a) XRD patterns of NiO and NiO/PCNT composite. (b) TGA curve of NiO/PCNT composite.

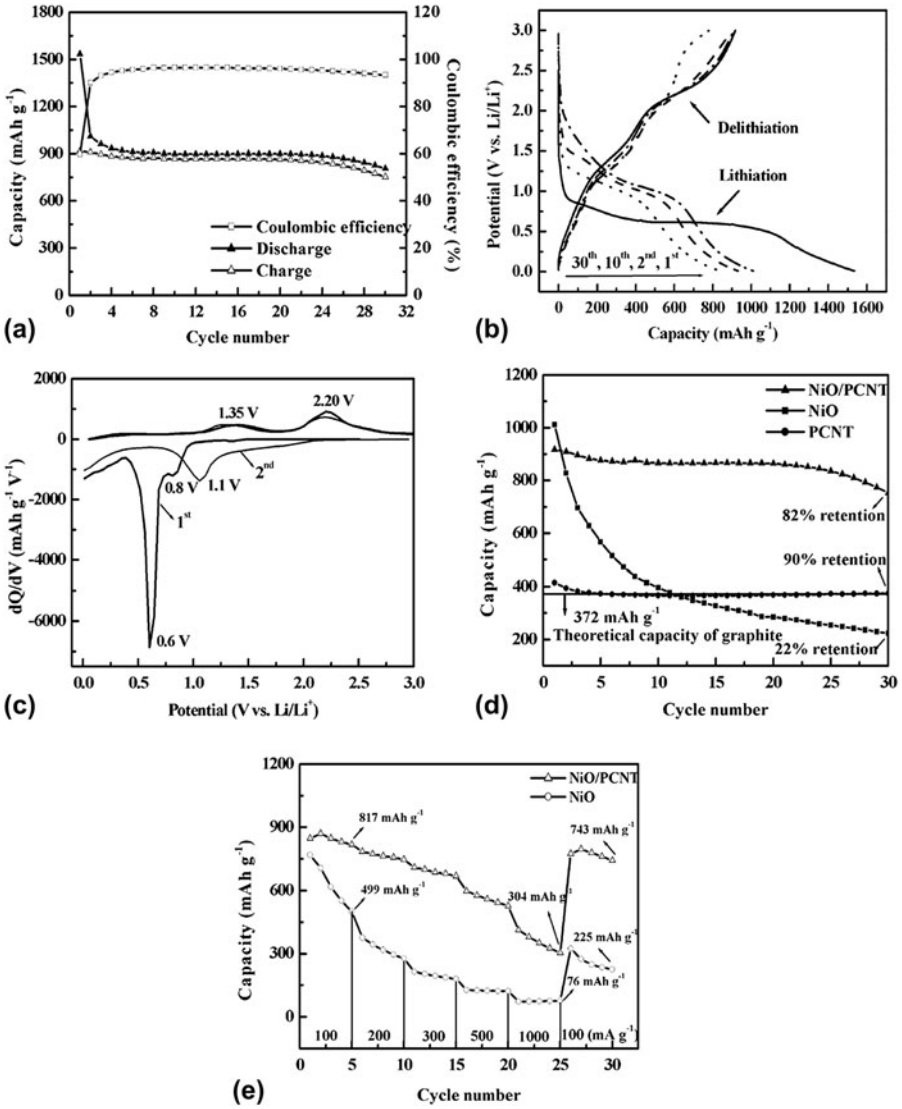


FIG. 4. (a) Cycling performance of NiO/PCNT composite at a current density of 100 mA/g. (b) Discharge/charge voltage profile of NiO/PCNT composite at a current density of 100 mA/g. (c) Differential capacity curves of NiO/PCNT composite at a current density of 100 mA/g. (d) Comparison of cycling performance of pure NiO, PCNT, and NiO/PCNT composite at a current density of 100 mA/g. (e) Rate performance of pure NiO and NiO/PCNT composite at various rates. The rates are indicated in Fig. 4(e) and the unit is milliampere per gram.

https://doi.org/10.1557/jmr.2013.227 Published online by Cambridge University Press

possesses good mechanical integrity and thus ensures good electrical connectivity between NiO and PCNT. Conductive PCNTs function as the structural support for effective utilization of NiO and as the conductive phase for fast charge transfer. Additionally, abundant pores on the surface of the NiO/PCNT microwire and between NiO/PCNT microwires provide large electrolyte/electrode interface and short diffusion path for electrons and electrolyte ions, as well as lots of buffering spaces for releasing the internal stress caused by lithiation/delithiation-induced volume change upon cycling. Based on the above merits, the performance of NiO/PCNT may be superior to that of pure NiO. To prove this hypothesis, electrochemical properties of pure NiO, PCNT, and NiO/PCNT anodes for LIBs are compared in a potential range of 0.01–3.0 V versus Li/Li^+. Figure 4(a) displays cycling performance of the NiO/PCNT composite at a constant current density of 100 mA/g. The composite shows high initial discharge and charge capacities of 1533 and 917 mAh/g, respectively, with a Coulombic efficiency of 60%. Low initial efficiency is attributed to solid–electrolyte interface (SEI) formation and electrolyte decomposite,[30] which is still a challenge to most anode materials.[30–33] From the second cycle, the capacity of the composite has small variation with obviously improved Coulombic efficiency of around 90–97%. After 30 cycles, the discharge and charge capacities still remain at 806 and 752 mAh/g, indicating good cycleability of the composite.

Figure 4(b) represents the 1st, 2nd, 10th, and 30th discharge/charge profiles of the NiO/PCNT composite at a current density of 100 mA/g. During the first cycle, a large capacity loss (616 mAh/g) can be found, which may be mainly ascribed to both SEI formation and electrolyte decomposition. In the range of 2–30 cycles, discharge and charge curves for each cycle are similar to each other, implying the greatly enhanced reversibility of electrochemical reactions due to the formation of SEI.

To investigate the reaction mechanism of the NiO/PCNT composite, differential capacity profiles that are derived from the 1st and 2nd discharge/charge profiles [Fig. 4(b)] are shown in Fig. 4(c). These curves clearly reflect structural transformations of NiO/PCNT during lithiation and delithiation process. In the first cycle, two cathodic peaks near 0.8 and 0.6 V, are related with the SEI formation (Li^+ + electrolyte + $e^- \rightarrow$ SEI) and the reduction of $Ni^{2+}O$ to Ni^0 ($NiO + 2Li^+ + 2e^- \rightarrow Ni + Li_2O$), respectively. Two anodic peaks at 1.35 and 2.20 V correspond to the partial dissolution of the organic SEI layer and the oxidation of Ni^0 ($Ni + Li_2O \rightarrow NiO + 2Li^+ + 2e^-$), respectively. These potential values have good resemblance to those of the reported NiO.[31,34,35] In the subsequent cycle, the cathodic peak near 0.6 V shifts to a high potential (1.1 V) and anodic peaks still retain the initial potential, indicating the improvement of electrochemical reversibility of the composite.[36]

To understand the effect of PCNT in the composite on lithium storage, cycling performance of pure NiO, PCNT, and NiO/PCNT composite is compared under the same conditions. As shown in Fig. 4(d), a clear difference in capacity retention can be seen from the repeated cycles. NiO/PCNT composite exhibits an initial reversible capacity of 917 mAh/g and then retains around 752 mAh/g over 30 cycles with 82% capacity retention, revealing good electrochemical stability. In contrast, pure NiO exhibits a worse capacity of 223 mAh/g over 30 cycles with low retention (22%). As for PCNT, its reversible capacity only slightly decreases from 414 to 374 mAh/g, corresponding to 90% capacity retention. By comparison, the composite has almost twice the theoretical capacity of graphite (372 mAh/g) and PCNT delivers a capacity almost equal to that of graphite, whereas pure NiO only has 40% that of graphite. Of note, the reversible capacity (752 mAh/g) of the composite even after 30 cycles is higher than the theoretical value of NiO (718 mAh/g). Such high capacity might be mainly due to four factors including capacitive properties of NiO, SEI formation, nano-size effect, and synergistic effect of 2D NiO nanosheet and 1D PCNT.[9,19,20,22,37,38] Accordingly, the introduction of PCNT into NiO is greatly helpful to improve the cycle performance of the electrode material.

The rate performance of pure NiO and NiO/PCNT composite at various current densities from 100 to 1000 mA/g is displayed to further confirm the positive effect of PCNT. The loading of active materials is about 0.5 mg. As seen in Fig. 4(e), charge capacities of pure NiO and the composite are 499 and 817 mAh/g at a low rate (100 mA/g) at the 5th cycle. When the rate is increased after 5 cycles in step up to a high rate (1000 mA/g), the composite still reaches a charge capacity of 304 mAh/g over 25 cycles, whereas pure NiO only retains 76 mAh/g with fast capacity fading. As the rate finally reverts to its initial value (100 mA/g), the composite and pure NiO retains 87.7% (743 mAh/g) and 29.3% (225 mAh/g) of initial charge capacity over 30 cycles, respectively. As expected, the composite has much higher capacity and better rate performance than pure NiO, indicating the potential of the composite in LIBs.

IV. CONCLUSIONS

Hierarchically porous NiO/PCNT composite is rationally constructed by using 1D and 2D nanocomponents and evaluated as an anode for LIBs. When used as anode materials for LIBs, the composite exhibits greatly enhanced reversible capacity (752 mAh/g after 30 cycles), cycleability (82% capacity retention after 30 cycles), and rate performance (817 mAh/g at 100 mA/g after 5 cycles; 304 mAh/g at 1000 mA/g after 25 cycles) compared to pure NiO. The improved lithium storage performance of NiO/PCNT composite may be benefited from the PCNT introduction and the attractive configuration made of different dimensional nanomaterials.

https://doi.org/10.1557/jmr.2013.227 Published online by Cambridge University Press

ACKNOWLEDGMENTS

This work was financially supported from Scientific Research Program of the Higher Education Institution of Xinjiang (Grant No. XJEDU2012I05), the National Natural Science Foundation of China (Grant No. 21063013), and the Scientific Research Starting Foundation for Doctoral Graduate, Xinjiang University (Grant No. 07020428024).

REFERENCES

1. V. Etacheri, R. Marom, R. Elazari, G. Salitra, and D. Aurbach: Challenges in the development of advanced Li-ion batteries: A review. *Energy Environ. Sci.* **4**, 3243 (2011).
2. J. Cabana, L. Monconduit, D. Larcher, and M.R. Palacin: Beyond intercalation-based Li-ion batteries: The state of the art and challenges of electrode materials reacting through conversion reactions. *Adv. Mater.* **22**, E170 (2010).
3. M.M. Thackeray, C. Wolverton, and E.D. Isaacs: Electrical energy storage for transportation-approaching the limits of, and going beyond, lithium-ion batteries. *Energy Environ Sci.* **5**, 7854 (2012).
4. V. Aravindan, J. Gnanaraj, Y.S. Lee, and S. Madhavi: $LiMnPO_4$-a next generation cathode material for lithium-ion batteries. *J. Mater. Chem.* 2013, **1**, 3518.
5. N.S. Choi, Z.H. Chen, S.A. Freunberger, X.L. Ji, Y.K. Sun, K. Amine, G. Yushin, L.F. Nazar, J. Cho, and P.G. Bruce: Challenges facing lithium batteries and electrical double-layer capacitors. *Angew. Chem. Int. Ed.* **51**, 9994 (2012).
6. M.Y. Ge, J.P. Rong, X. Fang, and C.W. Zhou: Porous doped silicon nanowires for lithium ion battery anode with long cycle life. *Nano Lett.* **12**, 2318 (2012).
7. P. Poizot, S. Laruelle, S. Grugeon, L. Dupont, and J.M. Tarascon: Nano-sized transition-metal oxides as negative-electrode materials for lithium-ion batteries. *Nature* **407**, 496 (2000).
8. B. Wang, J.L. Cheng, Y.P. Wu, D. Wang, and D.N. He: Porous NiO fibers prepared by electrospinning as high performance anode materials for lithium ion batteries. *Electrochem. Commun.* **23**, 5 (2012).
9. V. Aravindan, P.S. Kumar, J. Sundaramurthy, W.C. Ling, S. Ramakrishna, and S. Madhavi: Electrospun NiO nanofibers as high performance anode material for Li-ion batteries. *J. Power Sources* **227**, 284 (2013).
10. Y.N. Nuli, P. Zhang, Z.P. Guo, H.K. Liu, J. Yang, and J.L. Wang: Nickel-cobalt oxides/carbon nanoflakes as anode materials for lithium-ion batteries. *Mater. Res. Bull.* **44**, 140 (2009).
11. Q.M. Pan, L.M. Qin, J. Liu, and H.B. Wang: Flower-like ZnO–NiO–C films with high reversible capacity and rate capability for lithium-ion batteries. *Electrochim. Acta* **55**, 5780 (2010).
12. Y. Xia, W.K. Zhang, Z. Xiao, H. Huang, H.J. Zeng, X.R. Chen, F. Chen, Y.P. Gan, and X.Y. Tao: Biotemplated fabrication of hierarchically porous NiO/C composite from lotus pollen grains for lithium-ion batteries. *J. Mater. Chem.* **22**, 9209 (2012).
13. M.Y. Cheng and B.J. Hwang: Mesoporous carbon-encapasulated NiO nanocomposite negative electrode materials for high-rate Li-ion battery. *J. Power Sources* **195**, 4977 (2010).
14. T. Li, S.B. Ni, X.H. Lv, X.L. Yang, and S. Duan: Preparation of NiO-Ni/natural graphite composite anode for lithium ion batteries. *J. Alloys Compd.* **553**, 167 (2013).
15. M.M. Rahman, S.L. Chou, C. Zhong, J.Z. Wang, D. Wexler, and H.K. Liu: Spray pyrolyzed NiO–C nanocomposite as an anode material for the lithium-ion battery with enhanced capacity retention. *Solid State Ionics* **180**, 1646 (2010).
16. H.W. Lu, D. Li, K. Sun, Y.S. Li, and Z.W. Fu: Carbon nanotube reinforced NiO fibers for rechargeable lithium batteries. *Solid State Sci.* **11**, 982 (2009).
17. I.R.M. Kottegoda, N.H. Idris, L. Lu, J.Z. Wang, and H.K. Liu: Synthesis and characterization of graphene-nickle oxide nanostructures for fast charge-discharge application. *Electrochim. Acta* **56**, 5815 (2011).
18. Y.J. Mai, S.J. Shi, D. Zhang, Y. Lu, C.D. Gu, and J.P. Tu: NiO-graphene hybrid as an anode material for lithium ion batteries. *J. Power Sources* **204**, 155 (2012).
19. X.J. Zhu, J. Hu, H.L. Dai, and L. Jiang: Reduced graphene oxide and nanosheet-based nickel oxide microsphere composite as an anode material for lithium ion batteries. *Electrochim. Acta* **64**, 23 (2012).
20. C.H. Xu, J. Sun, and L. Gao: large scale synthesis of nickel oxide/multiwalled carbon nanotube composites by direct thermal decomposition and their lithium storage properties. *J. Power Sources* **196**, 5138 (2011).
21. S.G. Hwang, G.O. Kim, S.R. Yun, and K.S. Ryu: NiO nanoparticles with plate structure growth on graphene as fast charge-discharge anode materials for lithium ion batteries. *Electrochim. Acta* **78**, 406 (2012).
22. G.M. Zhou, D.W. Wang, L.C. Yin, N. Li, F. Li, and H.M. Cheng: Oxygen bridges between NiO nanosheets and graphene for improvement of lithium storage. *ACS Nano* **6**, 3214 (2012).
23. J.Z. Fan, H.Y. Mi, Y.L. Xu, and B. Gao: In situ fabrication of Ni $(OH)_2$ nanofibers on polypyrrole-based carbon nanotubes for high-capacitance supercapacitors. *Mater. Res. Bull.* **48**, 1342 (2013).
24. P. Palanisamy and A.M. Raichur: Synthesis of spherical NiO nanoparticles through a novel biosurfactant mediated emulsion technique. *Mater. Sci. Eng., C* **29**, 199 (2009).
25. Q.Y. Li, R.N. Wang, Z.R. Nie, Z.H. Wang, and Q. Wei: Preparation and characterization of nanostructured $Ni(OH)_2$ and NiO thin films by a simple solution growth process. *J. Colloid Interface Sci.* **320**, 254 (2008).
26. C.S. Shi, G.Q. Wang, N.Q. Zhao, X.W. Du, and J.J. Li: NiO nanotubes assembled in pores of porous anodic alumina and their optical absorption properties. *Chem. Phys. Lett.* **454**, 75 (2008).
27. M.K. Song, S.J. Par, F.M. Alamgir, J. Cho, and M.L. Liu: Nanostructured electrodes for lithium-ion and lithium-air batteries. The latest developments, challenges, and perspectives. *Mater. Sci. Eng., R* **72**, 203 (2011).
28. A. Kalam, A.S. Al-Shihri, A.G. Al-Sehemi, N.S. Awwad, G.H. Du, and T. Ahmad: Effect of pH on solvothermal synthesis of β-$Ni(OH)_2$ and NiO nano-architectures: Surface area studies, optical properties and adsorption studies. *Superlattice Microstruct.* **55**, 83 (2013).
29. C.M. Yang, C. Weidenthaler, B. Spliethoff, M. Mayanna, and F. Schuth: Facile template synthesis of ordered mesoporous carbon with polypyrrole as carbon precursor. *Chem. Mater.* **17**, 355 (2005).
30. X. Chen, N.Q. Zhang, and K.N. Sun: Facile ammonia-induced fabrication of nanoporous NiO films with enhanced lithium-storage properties. *Electrochem. Commun.* **20**, 137 (2012).
31. H. Wu, M. Xu, H.Y. Wu, J.J. Xu, Y.L. Wang, Z. Peng, and G.F. Zheng: Aligned NiO nanoflake arrays grown on copper as high capacity lithium-ion battery anodes. *J. Mater. Chem.* **22**, 19821 (2012).
32. D. Xie, W.W. Yuan, Z.M. Dong, Q.M. Su, J. Zhang, and G.H. Du: Facile synthesis of porous NiO hollow microspheres and its electrochemical lithium-storage performance. *Electrochim. Acta* **92**, 87 (2013).
33. A. Débart, L. Dupont, P. Poizot, J.B. Lerichen, and J.M. Tarascon: A transmission electron microscopy study of the reactivity mechanism of tailor-made CuO particles toward lithium. *J. Eletrochem. Soc.* **148**, A1266 (2001).
34. B. Varghese, M.V. Reddy, Y. Zhu, C.S. Lit, T.C. Hoong, G.V. Subba Rao, B.V.R. Chowdari, A.T.S. Wee, C.T. Lim, and C.H. Sow: Fabrication of NiO nanowall electrodes for high performance lithium ion battery. *Chem. Mater.* **20**, 3360 (2008).

https://doi.org/10.1557/jmr.2013.227 Published online by Cambridge University Press

35. X.H. Huang, J.P. Tu, B. Zhang, C.Q. Xhang, Y. Li, Y.F. Yuan, and H.M. Wu: Electrochemical properties of NiO–Ni nanocomposite as anode material for lithium ion batteries. *J. Power Sources* **161**, 541 (2006).
36. X.G. Liu, S.W. Or, C.G. Jin, Y.H. Lv, C. Feng, and Y.P. Sun: NiO/C nanocapsules with onion-like carbon shell as anode material for lithium ion batteries. *Carbon* **60**, 215 (2013).
37. Y.Q. Zou and Y. Wang: NiO nanosheets grown on graphene nanosheets as superior anode materials for Li-ion batteries. *Nanoscale* **3**, 2615 (2011).
38. S.Q. Ci, J.P. Zou, G.S. Zeng, Q. Sheng, S.L. Luo, and Z.H. Wen: Improved electrochemical properties of single crystalline NiO nanoflakes fro lithium storage and oxygen electroreduction. *RSC Adv.* **2**, 5185 (2012).

https://doi.org/10.1557/jmr.2013.227 Published online by Cambridge University Press